New relationships connecting a class of fractal objects and fractional integrals in space

Article *in* Fractional Calculus and Applied Analysis · December 2013

DOI: 10.2478/s13540-013-0056-1

VERSITA

Fractional Calculus & Applied Analysis
An International Journal for Theory and Applications
VOLUME 16, NUMBER 4 (2013)
(Print) ISSN 1311-0454
(Electronic) ISSN 1314-2224

SURVEY PAPER

NEW RELATIONSHIPS CONNECTING A CLASS OF FRACTAL OBJECTS AND FRACTIONAL INTEGRALS IN SPACE

Raoul R. Nigmatullin [1], **Dumitru Baleanu** [2,3,4]

Abstract

Many specialists working in the field of the fractional calculus and its applications simply replace the integer differentiation and integration operators by their non-integer generalizations and do not give any serious justifications for this replacement. What kind of "Physics" lies in this mathematical replacement? Is it possible to justify this replacement or not for the given type of fractal and find the proper physical meaning? These or other similar questions are not discussed properly in the current papers related to this subject. In this paper new approach that relates to the procedure of the averaging of smooth functions on a fractal set with fractional integrals is suggested. This approach contains the previous one as a partial case and gives new solutions when the microscopic function entering into the structural-factor does not have finite value at $N \gg 1$ (N is number of self-similar objects). The approach was tested on the spatial Cantor set having M bars with different symmetry. There are cases when the averaging procedure leads to the power-law exponent that does not coincide with the fractal dimension of the self-similar object averaged. These new results will help researches to understand more clearly the meaning of the fractional integral. The limits of applicability of this approach and class of fractal are specified.

MSC 2010: Primary 28A80, 26A33; Secondary 60G18, 26A30, 28A78

pp. xxx–xxx , DOI: 10.2478/s13540-013-0056-1

Springer

Key Words and Phrases: fractal object, self-similar object, spatial fractional integral, averaging of smooth functions on spatial fractal sets, Cantor set

1. Introduction and formulation of the problem

During the last two decades it became obvious that consideration of the properties of a fractal object (both in space and in time) needs a special mathematical tool. One of the efficient tools of such kind became the mathematics of the fractional calculus. Now this point of view is supported by many researches and the abbreviation FDA (Fractional Derivatives and its Applications) received a very wide propagation in the scientific world. Starting from the 90^{th} of the last century up to nowadays we have thousands publications, many workshops, exhibitions and conferences that are absorbed by the acronym FDA. For beginners one can recommend some monographs [14, 1, 12, 15, 13] and reviews [3, 4] including extended old and recent historical surveys, where the foundations of this "hot spot" are explained. The recent progress of the fractional calculus applications in dielectric spectroscopy one can find in [2]. One of the basic problems that did not accurately solved yet in the fractional calculus community is the finding of the desired relationship between the smoothed functions averaged over fractal objects and fractional operators. This problem was solved for the time-dependent functions averaged over Cantor sets in monograph [5] and paper [6], where the influence of unknown log-periodic function (leading finally to the understanding of the meaning of the fractional integral with the complex-conjugated power-law exponents) was taken into account. Possible generalizations helping to understand the role of a spatial fractional integral as a mathematical operator replacing the operation of averaging of the smoothed functions over fractal objects were considered in monograph [5] also. But in order to receive as a generalization the desired expressions for the gradient, divergence and curl expressed by means of the fractional operator in the limits of mesoscale (when the current scale η lies in the interval ($\lambda < \eta < \Lambda$) determining the limits of a possible self-similarity) it was necessary to apply the additional averaging procedure over possible places of location of the fractal object considered. This procedure provides the correct convergence of the microscopic function $f(z)$ on small $\eta \leq \lambda$ and large $\eta \leq \Lambda$ scales. But the basic reason that serves as a specific mathematical obstacle in accurate establishing of the desired relationship between the fractal object and the corresponding fractional integral is the absence of the 2D- and 3D-Laplace transformations. Application of the Fourier transform replacing the absence of the (2,3)D-Laplace transformation leads mathematically to the fact that the behavior of the trigonometric functions on large scales becomes uncertain and the limit of the function

$$\lim_{N \gg 1} \exp(i\mathbf{kr}\xi^N) =? \tag{1}$$

at $\xi > 1$ does not exist in the conventional sense. In order to provide the convergence of the limit (1) at conditions ($N \gg 1, \xi > 1$) the additional averaging procedure over possible places of location of the fractal object was applied [5]. So, the finding of the correct mathematical procedure that helps to overcome the ambiguity of expression (1) is the actual problem in establishing the desired "bridge" between fractal geometry and fractional calculus.

In this paper we want to demonstrate another approach that can link the procedure of the averaging of a smooth function for a certain class of the given self-similar objects with the fractional integral and its possible generalizations in space. This alternative approach helps to solve this problem in more accurate form and demonstrates new possibilities that can exist between fractals and fractional integrals in space.

The content of this paper is organized as follows. Section **2** is devoted to calculation of the self-similar 1D product (structure-factor) that serves a main link between the smoothed function and the fractal object considered. In Section **3** we realize the numerical test for 1D spatial Cantor set containing M bars and its possible modifications. In Section **4** we consider another class of fractal objects when the results obtained in Section **2** can be applicable for more complex cases. The last Section **5** summarizes the basic results and outlines the perspectives of application of new approach for solution of similar problems in the mathematical physics of the fractional calculus. Besides, the basic results of this approach helps to find at least three distributions that remain invariant relatively scaling transformations.

2. Mathematical part: Properties of the 1D self-similar product

As well-known earlier [12, 5], for many fractal objects located in a space the most convenient procedure for their description is based on the following property of the Fourier transform

$$f(\mathbf{r}) = \int_{-\infty}^{\infty} F(\mathbf{k}) \exp(i\mathbf{kr}) d^3\mathbf{k} =: F(\mathbf{k}), \;\; f(\mathbf{r} + \mathbf{a}) := \exp(i\mathbf{ka}) F(\mathbf{k}). \tag{2}$$

This property helps to segregate the Fourier image of the averaged smooth function (presented by the function $F(\mathbf{k})$ in 3D-Fourier space) from the structure-factor, which shows the location of the fractal object in space. The current generation of a fractal object can be expressed with the help of a "star" of the $\boldsymbol{k}$-vector $(\boldsymbol{k}_1, \cdots, \boldsymbol{k}_r)$, where r determines a finite number of new self-similar objects that are created on the current stage of the desired fractal object and vector $\mathbf{a}(\mathbf{a}_1, \mathbf{a}_2, \cdots, \mathbf{a}_r)$ shows the directions of the location of the current generation of the given fractal in space. Based on the property (2) it is easy to see that from the mathematical point of view it becomes necessary to consider the product (presenting itself a general definition of the structure-factor) of the following form

$$P(z_1, z_2, \ldots, z_r) = \prod_{n=-N}^{n=N} f(z_1\,{\xi_1}^n, \ldots, z_r\,{\xi_r}^n), \quad z_q = k\Lambda\cos(\theta_q), \quad q = 1, 2, \cdots, r. \tag{3}$$

In the expression (3) the value k defines the modulus of the wave-vector, Λ is the value of the vector referring to the initial (the largest for the case $\xi < 1$ and vice versa) fractal object, θ_q is a set of angles between vectors $\mathbf{k}_q$ and Λ, respectively. The value ξ defines the scaling parameter. For self-affine fractals having different symmetry it cannot be the same.

So, the basic problem from the mathematical point of view can be formulated as follows. To consider the properties of the product (3) and relate these properties with some types of the fractional integrals that are considered (for example, in the book [1]) and accepted in the fractional calculus as basic definitions.

As it follows from (3) the consideration of a simple self-similar 1D-object in space is closely related to consideration of the mathematical properties of the product

$$P(z) = \prod_{n=-N_0}^{N} b^n f(z\xi^n). \tag{4}$$

The self-similar properties of sums compared from fractal units are considered recently in our paper [11]. The product (4) is closely related to the structure-factor for simple fractals considered in [5] that indicates the location of the fractal studied in 3D space. Here b and ξ determine the scaling parameters, the variable z can accept real or complex values (for example, it can coincide with dimensionless Laplace variable variable $(z = i\omega + s)$ or with the Fourier parameter $(i(\mathbf{ka}))$ in space. Here we consider more general case when the lower limit N_0 does not coincide with upper limit N. For distinctness we put $(N_0 < N)$. Making a substitution $z \to z\xi$ in (4), we obtain the following identity

$$P(z\xi) = \prod_{n=-N_0}^{N} b^n f(z\xi^{n+1}) = \frac{1}{b}\prod_{n=-N_0+1}^{N+1} b^n f(z\xi^n) = b^{N-|N_0|}\frac{f(z\xi^{N+1})}{f(z\xi^{-N_0})}P(z). \tag{5}$$

If the microscopic function $f(z)$ describing the dynamic process or geometrical location of an elementary fractal on mesoscale is finite for large and small values of variable z (as it was supposed in [5, 6] and other papers

[7, 8]) then at $N = \mid N_0 \mid$ and in the limit $N \gg 1$ one can obtain (for distinctness we put $\xi > 1$) the following scaling equation

$$P(z\xi) = \frac{A}{c_0}P(z), \;\; f(z) = A, \;\text{for}\;\; \mid z \gg 1 \mid, \;\text{and}\; f(z) = c_0, \;\text{for}\;\; \mid z \ll 1 \mid \tag{6}$$

with the well-known solution [5, 6]

$$\begin{gathered} P(z) = PR_\nu(ln(z)) \cdot z^\nu, \quad \nu = \frac{lnA/c_0}{ln(\xi)}, \\ PR_\nu(ln(z) \pm ln(\xi)) = PR_\nu(lnz). \end{gathered} \tag{7}$$

Here the expression $PR_\nu(ln(z))$ defines the unknown log-periodic function. The main question can be formulated as follows: how to find the solution for product (4) satisfying the functional equation (6) when the asymptotic behavior of the microscopic function $f(z)$ is not finite or does not exist? Mathematically this condition can be expressed as

$$\lim_{N \gg 1} f(z) = \{ \begin{matrix} \text{does not exist} \\ \infty \end{matrix} . \tag{8}$$

The first row in (8) can be associated with condition (2). In order to find the solution of the functional equation (6) at condition (8), we present identity (5) in the form

$$L(z\xi) = L(z) + \Phi(z\xi^{n+1}) - \Phi(z\xi^{-N_0}) + B, \tag{9}$$

where

$$L(z) = ln[P(z)], B = (N - N_0)ln(b), \Phi(z) = ln[f(z)]. \tag{10}$$

In the equations (8), (9) and below the value N_0 is considered as a positive value. At $N = N_0$, $B = 0$. For distinctness we put $\xi > 1$. We should note here that the case $\xi < 1$ is reproduced from expressions (7), (9), (10) and expressions below (containing the parameter $\xi > 1$) by simple replacement $\xi \to \frac{1}{\xi}$. From identity (9) by the replacement $z \to z\xi^{q-1}$, we obtain easily

$$L(z\xi^q) = L(z\xi^{q-1}) + \Phi(z\xi^{N+q}) - \Phi(z\xi^{-N_0+q-1}) + B, q = 1, 2, ..., k-1, k, \dots . \tag{11}$$

Taking into account condition (8) we cannot eliminate the large term $\Phi(z\xi^{N+q})$ from (11). So, in general the infinite set of equations (10) contains two types of different variables $L(z\xi^q), \Phi(z\xi^{N+q})$ $(q = 1, 2, ..., k, ...)$ and cannot be reduced to the system containing only one type of variable. In order to close the infinite chain of equations (11) relatively unknown function L(z) (or equally for the unknown microscopic function $\Phi(z)$) we make the reasonable supposition (it will be justified below numerically and analytically)

$$\Phi(z\xi^{N+k}) \cong \sum_{q=1}^{k-1} w_q \Phi(z\xi^{N+q}). \tag{12}$$

Here $\{w_q\}$ $(q = 1, 2, \cdots, k-1)$ determines a set of constants that approximate the function figuring on the left-hand side. These constants can be found numerically with the help of the linear-least square method (LLSM). From the system of equations (11) we have

$$\Phi(z\xi^{N+q}) = L(z\xi^q) - L(z\xi^{q-1}) + Lm_q - B, \; q = 1, 2, \cdots, k-1, \tag{13}$$

$$\Phi(z\xi^{-N_0+q-1}) \cong Lm_q, \text{ for } 1 \ll N_0 \preceq N. \tag{14}$$

Here we took into account the limit (6) describing approximately the behavior of $f(z)$ at small values of the variable z. For $q = k$ from (13) we have

$$\begin{gathered} L(z\xi^{k-1}) - Lm_k + B + \Phi(z\xi^{N+k}) = L(z\xi^k), \\ \Phi(z\xi^{-N_0+k-1}) \cong Lm_k, \; 1 \ll N_0 \preceq N. \end{gathered} \tag{15}$$

Taking into account the approximate decoupling (12) and relationships (13) we obtain

$$\begin{aligned} L(z\xi^k) - L(z\xi^{k-1}) + Lm_k - B = \Phi(z\xi^{N+k}) \cong \sum_{q=1}^{k-1} w_q \Phi(z\xi^{N+q}) \\ = \sum_{q=1}^{k-1} w_q [L(z\xi^q) - L(z\xi^{q-1})] + \sum_{q=1}^{k-1} w_q (Lm_q - B). \end{aligned} \tag{16}$$

After some simple algebraic transformations of expression (16) we obtain finally the closed functional equation with respect to the remaining variable $L(z)$

$$\begin{gathered} L(z\xi^k) = (1 + w_{k-1}) L(z\xi^{k-1}) + \sum_{q=1}^{k-2} (w_q - w_{q+1}) L(z\xi^q) - w_1 L(z) + R, \\ R = \sum_{q}^{k-1} w_q (Lm_q - B) - (Lm_k - B). \end{gathered} \tag{17}$$

So, the solutions of the functional equation (17) help to find new expressions for the product (4) when the condition (8) is satisfied. The solutions of (17) are closely related with the values of the roots of polynomial

$$P(\lambda) = \lambda^k - (1 + w_{k-1})\lambda^{k-1} - \sum_{q=1}^{k-2} (w_q - w_{q+1})\lambda^q - w_1 = 0. \tag{18}$$

If the roots of (18) are different, then the general solution of the functional equation (17) can be presented in the form (see Sect. **6**, Mathematical Appendix)

$$L(z) = \sum_{s=1}^{k} PR_s(lnz)\, z^{\nu_s} + C(R). \tag{19}$$

Here $C(\mathrm{R})$ is a constant that is found by an arbitrary constant variation method and the set of the power-law exponents $\nu_s(s = 1, 2, \cdots, k)$ is defined as

$$\nu_s = \frac{ln(\lambda_s)}{ln(\xi)} \quad (\xi \succ 1). \tag{20}$$

The set of $PR_s(ln(z))$ from (19) determines the unknown log-periodic functions. These functions can be decomposed into the infinite Fourier series

$$PR_s(lnz) = A_0^{(s)} + \sum_{k=1}^{\infty} \left[Ac_k^{(s)} \cos\left(2\pi k \tfrac{ln(z)}{ln(\xi)}\right) + As_k^{(s)} \sin\left(2\pi k \tfrac{ln(z)}{ln(\xi)}\right)\right],$$
$$PR_s(lnz \pm ln(\xi)) = PR_s(lnz), \tag{21}$$

with period $ln(\xi)$. The decomposition coefficients of the series (21) should be found from initial or some a priori conditions (when the parameter ξ is supposed to be known). When some root ν_s figuring in (20) accepts the negative value, then (as it has been shown in [9]) it is necessary to replace the root by its modulus value and the log-periodic function in (19) should be replaced by some anti-periodic function having the following decomposition

$$PR_s^{(a)}(ln(z)) = \sum_{k=1}^{\infty} \left[Ac_k^{(s)} \cos\left(\pi k \tfrac{ln(z)}{ln(\xi)}\right) + As_k^{(s)} \sin\left(\pi k \tfrac{ln(z)}{ln(\xi)}\right)\right],$$
$$PR_s^{(a)}(ln(z) \pm ln(\xi)) = -PR_s^{(a)}(ln(z)). \tag{22}$$

As reminded above, the constant figuring in (19) is determined by the arbitrary constant variation method and depends totally on the constant value R from (17). If one of the roots of the polynomial (18) ν_g is degenerated, then the solution for this root is written in the form

$$L_g(z) = \left[\sum_{r=1}^{g} PR_r(ln(z))(ln(z))^{r-1}\right] z^{\nu_g}, \;\; \nu_g = \frac{ln(\lambda_q)}{ln(\xi)}, \;\; \xi > 1, \tag{23}$$

where the value g determines the degree of degeneracy. Here, again the unknown log-periodic functions entering into (23) are determined by decompositions (21) or (22). If we take into account relationship (10), then one can obtain the solution for the product *P(z)*. It is useful also to give the solution of (17) for the case when a couple of the roots in (18) is complex-conjugated,

$$\nu = Re(\nu) \pm iIm(\nu) = \frac{ln(Re\lambda \pm iIm\lambda)}{ln(\xi)},$$

$$L(z) = z^{Re(\nu)} \left[A_0 + \sum_{k=1}^{\infty} \left(Ac_k \cos(\tfrac{2\pi k}{ln(\xi)} lnz + (Im\nu)\ lnz) \right) \right]$$
$$+ z^{Re(\nu)} \left[\sum_{k=1}^{\infty} \left(As_k \sin(\tfrac{2\pi k}{ln(\xi)} lnz + (Im\nu)\ lnz) \right) \right]. \quad (24)$$

Here we want to demonstrate some general properties of the functional equation (17) and its corresponding polynomial (18).

A direct test shows that the polynomial (18) has always the root $\lambda = 1$ and so it can be decomposed as

$$P(\lambda) = (\lambda - 1) \left(\lambda^{k-1} - w_{k-1}\lambda^{k-2}, - \cdots, -w_1 \right). \quad (25)$$

If the functions defined by relation (10)

$$f(z\xi^{N+q}) = \exp\left(\Phi(z\xi^{N+q}) \right),\ q = 1, 2, \cdots, k-1, \quad (26)$$

have negative values then from decoupling procedure (12) it follows

$$f(z\xi^{n+k}) = \prod_{q=1}^{k-1} f(z\xi^{N+q})^{w_q}. \quad (27)$$

Taking the imaginary part from both parts of (27) we have

$$i\pi = \sum_{q=1}^{k-1} i\pi w_q \ \text{ or } \ \sum_{q=1}^{k-1} w_q = 1. \quad (28)$$

Condition (28) leads to the two-fold degeneracy of the root $\lambda = 1$ and for this case instead of decomposition (25) we have

$$P(\lambda) = (\lambda - 1)^2 \left(\lambda^{k-2} + a_{k-2}\lambda^{k-3} + \cdots + a_1 \right),$$
$$a_1 = w_1,\ a_2 = w_1 + w_2,\ \cdots,\ a_{k-2} = w_1 + w_2 + \cdots + w_{k-2}. \quad (29)$$

Before to start considering some interesting example, it is instructive to give the solution for some partial cases k=2, 3, 4. These cases admit analytical solutions. As we will see below, these cases can be met frequently in possible applications.

Case $k = 2$. Approximate decoupling (it follows from (11), $w_1 = 1$)

$$f(z\xi^{N+2}) \cong f(z\xi^{N+1}),\ \text{or}\ \Phi(z\xi^{N+2}) \cong \Phi(z\xi^{N+1}). \quad (30)$$

The functional equation

$$L(z\xi^2) - 2L(z\xi) + L(z) = R. \quad (31)$$

The desired polynomial and its roots

$$P(\lambda) = (\lambda - 1)^2 = 0. \quad (32)$$

The general solution of the functional equation (31)

$$L(z) = PR_1(lnz) + PR_2(lnz)ln(z) + k_2 ln^2(z),$$
$$k_2 = \tfrac{R}{2ln^2\xi}\,. \tag{33}$$

Case $k = 3$. For this case we suppose that the following approximate decoupling is satisfied

$$f(z\xi^{N+3}) \cong f(z\xi^{N+1})^{w_1} f(z\xi^{N+2})^{w_2}. \tag{34}$$

The functional equation

$$L(z\xi^3) - (1 + w_2)L(z\xi^2) - (w_1 - w_2)L(z\xi) + w_1 L(z) = R. \tag{35}$$

The desired polynomial and its roots

$$P(\lambda) = (\lambda - 1)(\lambda^2 - w_2\lambda - w_1) = 0, w_1 + w_2 \neq 1,$$

$$\lambda_{1,2} = \tfrac{w_2}{2} \pm \sqrt{(\tfrac{w_2}{2})^2 + w_1}. \tag{36}$$

The general solution of the functional equation (35) ($w_1 + w_2 \neq 1$):

$$L(z) = PR_0(lnz) + PR_1(lnz)z^{\nu_1} + PR_2(lnz)z^{\nu_2} + k_1 lnz,$$

$$\nu_{1,2} = \frac{ln(\lambda_{1,2})}{ln(\xi)}, k_1 = \frac{R}{ln(\xi)(1 - w_1 - w_2)}. \tag{37}$$

The general solution of the functional equation (34) ($w_1 + w_2 = 1$):

$$P(\lambda) = (\lambda - 1)^2(\lambda + w_1) = 0,$$
$$L(z) = PR_1(lnz) + PR_2(lnz)ln(z) + PR_3^{(a)}(lnz)z^{\nu_3} + k_2 ln^2 z,$$

$$\nu_3 = \frac{ln(\mid w_1 \mid)}{ln\xi}, k_2 = \frac{R}{2ln^2\xi(1 + w_1)}. \tag{38}$$

Case $k = 4$. We suppose that for this case the following approximate decoupling is valid

$$f(z\xi^{N+4}) \cong f(z\xi^{N+1})^{w_1} f(z\xi^{N+2})^{w_2} f(z\xi^{N+3})^{w_3}. \tag{39}$$

The functional equation

$$L(z\xi^4) - (1 + w_3)L(z\xi^3) - \Sigma_{q=1}^{2}(w_q - w_{q+1})L(z\xi^q) + w_1 L(z) = R. \tag{40}$$

The desired polynomial and its roots

$$P(\lambda) = (\lambda - 1)\left(\lambda^3 - w_3\lambda^2 - w_2\lambda - w_1\right) = 0.\ w_1 + w_2 + w_3 \neq 1. \tag{41}$$

The general solution of the functional equation (39) ($w_1 + w_2 + w_3 \neq 1$)

$$L(z) = PR_0(lnz) + \textstyle\sum_{s=1}^{3} PR_s(lnz)z^{\nu_s} + k_1 ln(z),$$
$$\nu_{1,2,3} = \frac{ln\lambda_{1,2,3}}{ln\xi},\ k_1 = \frac{R}{ln\xi(1 - w_1 - w_2 - w_3)}. \tag{42}$$

The general solution of the functional equation (40) $(w_1+w_2+w_3=1)$

$$P(\lambda)=(\lambda-1)^2\left(\lambda^2+(w_1+w_2)\lambda+w_1\right)=0,$$
$$L(z)=PR_1(lnz)+PR_2(lnz)ln(z)+\Sigma_{s=3}^{4}PR_s(lnz)z^{\nu_s}+k_2ln^2z,$$
$$k_2=\frac{R}{2ln^2\xi(1+2w_1+w_2)}. \tag{43}$$

In the expressions given above the log-periodic functions are defined by decompositions (21) and (22) for periodic and anti-periodic cases, correspondingly. The desired expressions for the product $P(z)$ are obtained from the solutions for $L(z)$ with the use of relationship (10). Solutions for the case $\xi<1$ are obtained from these expressions by simple replacement $\xi\rightarrow\frac{1}{\xi}$. We want to stress here the principle difference of appearance of the power-law exponents in expressions (7), (37) and (42) and a formal absence of the power-law behavior in expression (33). Besides this difference, we obtain the mixed dependence between power-law and logarithmic behavior in expressions (38) and (43).

Before it was accepted to consider that the power-law exponent is formed from the limiting values of the microscopic function (expression (7)). In the new expressions derived in this paper we can mark at least two new reasons of appearance of the power-law exponent when the condition (8) is fulfilled.

For the nondegenerate case $\Sigma_{q=1}^{k-1}w_q\neq 1$ the power-law exponent is formed from the value k_1 figuring in expressions (37), (42) while for the degenerate case $\Sigma_{q=1}^{k-1}w_q=1$ (expressions (33), (38) and (43)) in formation of the power-law exponent the constant A_0 from (21) plays the essential role. In these two new cases marked above the power-law exponent *does* not coincide with the fractal dimension of the geometrical object considered. In the conclusion of this section we want to give some additional arguments and determine some conditions justifying the decoupling supposition (12). Definitely, for each concrete form of the fractal considered the limits of applicability should be considered independently. The approximate relationship (12) represents itself the functional equation for the function $\Phi(z)$. If $N>>1$, then from this expression we obtain approximately the desired solution

$$\Phi(z\xi^N)\cong\left(\sum_{q=1}^{k-1}w_q\right)\Phi(z\xi^N),$$
$$\Phi(z)\cong PR_0(lnz),$$
$$\sum_{q=1}^{k-1}w_q=1. \tag{44}$$

Here $PR_0(lnz)$ is defined by decomposition (21). So, the decoupling (12) can be realized with high accuracy, if, in turn, the function $\Phi(z)$ can be approximated and finally replaced with high accuracy by log-periodic function determined by decomposition (21). If condition (44) is realized then (because of log-periodic properties of (21)) the condition (30) referring to Case 2 will be realized automatically. But we stress again that for each specific type of fractal condition (44) should be more accurately tested in order to find the limits of applicability.

3. Numerical test for Cantor set with M bars

As an example for testing of decoupling condition (12), we consider the classical Cantor set containing M bars in each stage of its generation. As it has been shown in the book [5] the structure-factor (defined above by the general expression (3) for the Cantor set containing M bars and located along OX axis is expressed as

$$P_{N_1}(x) = \prod_{n=-N_1}^{N-1} Re\left[\frac{1-\exp(ixM\xi^n)}{M(1-\exp(ix\xi^n))}\right] = \prod_{n=-N_1}^{N_1} f_M(x\xi^n),$$
$$x = ka,\ \xi > 1, \Phi_M(x) = ln(\mid f_M(x) \mid),\ L_{N_1}(x) = ln(\mid P_{N_1}(x) \mid). \quad (45)$$

For concrete calculations of this expression and testing the supposition (12) we chose the following values of the parameters entering into (45):

$$\xi = 1.5,\ N_1 = 50,\ x \in [0,1],\ M = 2,3,5. \quad (46)$$

The discrete number of points determining the interval of the current variable x was limited by three values of $N = 50$, 150 and 500. Calculations show that it is much convenient to test the value $L_{N_1}(x) = ln(P_{N_1}(x))$. The typical behavior of this function for $M = 5$, $N = 150$ is shown on Figure 1.

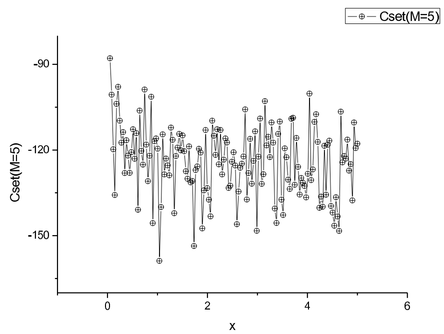

FIGURE 1. Typical behavior of the function $L_{N_1}(x_1) = ln(P_{N_1}(x))$ for $M = 5$ defined by expression (44). The values of parameters are collected in (45). Number of points $N = 150$. Interval of the variable x is [0.05-5.0].

All test calculations are divided into two steps:

Step 1. The verification of the supposition (11) (or equivalently the accuracy of the decomposition (44)) and calculation of the fitting parameters $\{w_q\}$.

Step 2. The final fitting of one of the functions (33), (37), (38), (42), (43) to the function $L_{N_1}(x)$ that depends essentially on the number of parameters $\{w_q\}$.

These calculations were realized for different number of Cantor bars having $M = 2, 3, 5$ and number of points $N = 50$, 150 and 500. The results of the verification of hypothesis (44) for the function $\Phi_M(x)$ ($M = 2, 3, 5$) are illustrated by Figures 2, 3 and 4 for N=50.

The value of the cutoff parameter K determining the upper limit of decomposition (21) and the value of the relative error (defined below by (50)) for different M and N are collected in Table 1.

The analysis shows that for relatively large values of $N_1 >> 1$ the supposition (43) is realized with relatively high accuracy (the value of the relative cannot exceed 1 (per/cent) or can be even less) for all tested N = 50, 150 and 500. The value of the constant R entering into expression (32) and calculated from (16) equals zero. So, the fitting function for the fractal object as the Cantor set is reduced (because of expression (44)) to the simplest Case k=2,

$$L(z) = PR_1(lnz) + PR_2(lnz)\ lnz. \tag{47}$$

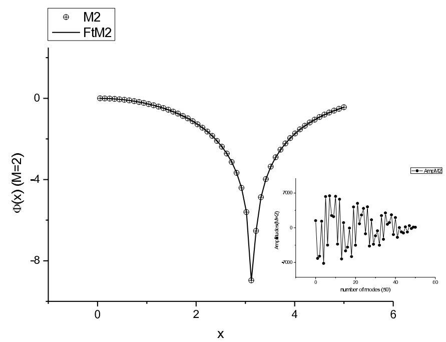

FIGURE 2. The verification of the hypothesis (43) for $M = 2$ ($N = 50$). The points correspond to the function $\Phi_2(x)$ and solid line corresponds to fit of log-periodic function from (20). In the small plot below the distribution of the amplitudes of the corresponding log-periodic function is shown.

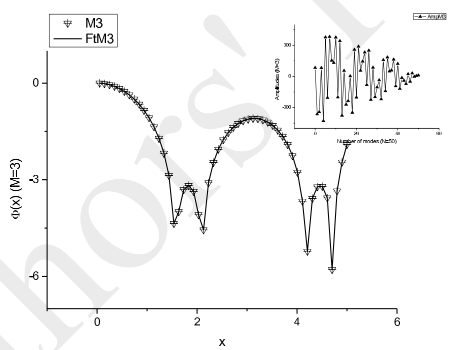

FIGURE 3. The verification of the hypothesis (43) for $M = 3$ ($N = 50$). The points correspond to the function $\Phi_3(x)$ and solid line corresponds to fit of the log-periodic function from (20). In the small plot above the distribution of the amplitudes of the log-periodic function for this case is shown.

Taking into account the relationships (21) it is convenient to present function (47) for the fitting purposes in the form

$$Lf(x) = A_0^{(2)} ln(x) + \sum_{k=1}^{K} Ac_k^{(2)} Cl_k(lnx) + \sum_{k=1}^{K} As_k^{(2)} Sl_k(lnx)$$
$$+A_0^{(1)} + \sum_{k=1}^{K} Ac_k^{(1)} C_k(ln(x)) + \sum_{k=1}^{K} As_k^{(1)} S_k(ln(x)),$$

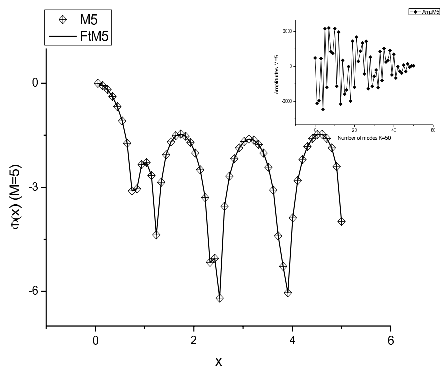

FIGURE 4. The verification of the hypothesis (43) for $M = 5$. The points correspond to the function $\Phi_5(x)$ and solid line corresponds to fit of the log-periodic function from (20). In the small plot above the distribution of the amplitudes of the log-periodic function for this case is shown. The values of the relative error for different $M = 2, 3, 5$ and $N = 50$ is collected in Table 1. For other values of $N = 150, 500$ the fit looks similar and so it is not shown. The values of the relative error for all these cases are collected in Table 1.

The number of bars M	The number of the generated points N	The value of the cutoff parameter K	The value of the relative error (%)
2	50	25	$6.161*10^{-5}$
3	50	25	$6.662*10^{-5}$
5	50	25	$6.671*10^{-5}$
2	150	50	0.14491
3	150	50	0.27107
5	150	50	0.09772
2	500	75	1.31705
3	500	75	0.79646
5	500	75	0.40202

TABLE 1. The value of the relative error calculated in testing of the hypothesis (44) $\Phi \cong PR_0(lnz)$. See the set of Figures 2, 3 and 4 for details.

$$C_k(ln(x)) = \cos(\tfrac{2\pi k}{ln\xi} ln(x)),\ S_k(ln(x)) = \sin(\tfrac{2\pi k}{ln\xi} ln(x)),$$

$$Cl_k(ln(x)) = (lnx)\cos(\tfrac{2\pi k}{ln\xi} ln(x)),\ Sl_k(ln(x)) = (lnx)\sin(\tfrac{2\pi k}{ln\xi} ln(x)). \quad (48)$$

The function (47) contains 2+4K fitting parameters. The cutoff parameter K is determined by the value of the relative error

$$RelErr(\%) = \left(\frac{stdev(L_{N_1}(x) - Lf(x))}{mean \mid L_{N_1}(x) \mid}\right) 100\%. \quad (49)$$

Here $Lf(x)$ implies the corresponding fitting function, the symbols stdev($f(x)$) and mean ($f(x)$) determine the conventional value of the standard deviation and expectation value, respectively. The results of the fitting of the function $L_{N_1}(x) = ln(P_{N_1})$ from (45) to function (48) are illustrated by Figures 5, 6, 7, 8 for $M = 2$ and $M = 5$, correspondingly. The results for $M = 3$ are not shown because they are similar. Analysis of these figures shows that for the accurate fitting the relatively large number of the fitting parameters entering into (48) is required. The accuracy of the fitting is decreased with increasing of the value of *N*. The calculated values of $A_0^{(2)}, RelErr(\%)$ at given *N*(K) are collected in Table 2. This simple test shows that decoupling supposition (12) (which is justified by the fit of expression (44)) to $\Phi_M(x)$ is very reasonable and can be applied for establishing the desired relationships between non-integer operators and fractals averaged with smooth functions in space. These results give new understanding of the fractal dimension and additional evidences that the relationship between the power-law exponent figuring in non-integer operator and power-law exponents appearing in Cases 2, 3, 4 considered above is not simple as it was supposed earlier.

4. Possible generalizations

How to generalize the results obtained in the previous section for more complex fractals? For example, if the Cantor set with $M = 2$ is obtained with the help of rotation operation realized along OZ-axis, then the structure-factor for this fractal having a continuous cylindrical symmetry is expressed as [5],

$$P_{N_1}(x) = \prod_{n=-N_1}^{N_1} \left(\tfrac{1}{2}(1 + J_0(x\xi^n))\right),\ x = \sqrt{k_x^2 + k_y^2}\,\lambda_{min}\,(1 - \xi^{-1}),$$
$$\xi > 1,\ \eta \in [\lambda_{min}, \Lambda_{max}]\, L_{N_1}(x) = ln(P_{N_1}(x)). \quad (50)$$

Here $J_0(x)$ is the classical Bessel function of the zeroth order. The scaling parameter ξ (it is equaled to $3/2$ for numerical calculations) is counted off from the minimal scale λ_{min}.

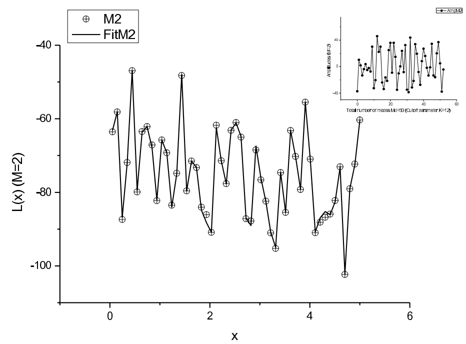

FIGURE 5. Verification of hypothesis (46) for $M = 2$ and $N = 50$. The function $L_{N_1}(x)$ from (44) is presented by crossed points. The fitting function (47) is presented by solid line. The distribution of amplitudes of the log-periodic function is shown above in the small frame.

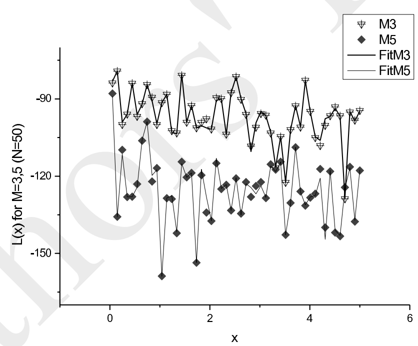

FIGURE 6. Verification of hypothesis (46) for $M = 3, 5$ and $N = 50$. The functions $L_{N_1}(x)$ from (44) are presented by crossed triangles and black rhombs, correspondingly. The fitting functions (47) are presented by solid lines. The distributions of amplitudes for these cases are not shown because they look similar to $M = 2$.

The similar test described above and applied to product (50) shows that Case k=2 is valid for this case also. So, for the fitting of the function $L_{N_1}(x) = ln(P_1(x))$ the hypothesis (46) is applicable again. Figure 9 demonstrates the results of the fitting of function (48) to $L_{N_1}(x)$ from (50)) for N=150 and K= 10. We should note here that in opposite to the first example the Bessel function $J_0(x)$ entering to the product (50) has the

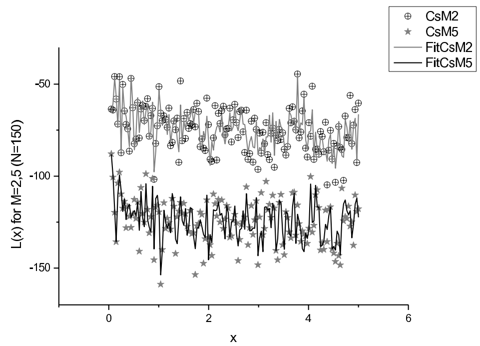

FIGURE 7. Verification of hypothesis (46) for $M = 2, 5$ and $N = 150$. The functions $L_{N_1}(x)$ from (44) are presented by crossed circles and grey stars, correspondingly. The fitting functions (47) are presented by solid lines. The distributions of amplitudes are not shown because they look similar to $M = 2$. Other parameters are collected in Table 2.

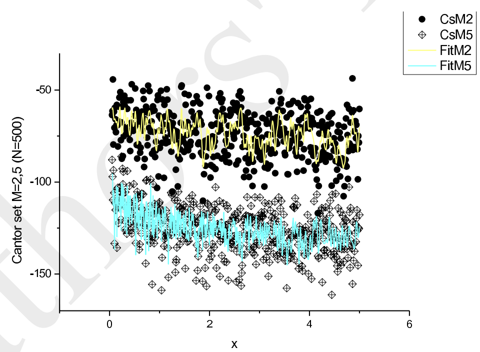

FIGURE 8. Verification of hypothesis (46) for $M = 2, 5$ and $N = 500$. The functions $L_{N_1}(x)$ from (44) are presented by dark circles and crossed rhombs, correspondingly. The fitting functions (47) are presented by yellow and blue lines. The fit of the Cantor set for M=3 and distributions of amplitudes are not shown because they look similar to $M = 2$. Other parameters are collected in Table 2.

finite limits for both cases

$$J_0(z) = 0, \text{ for } z \gg 1, \text{ and } J_0(0) = 1. \tag{51}$$

It means that the solution for (50) has the form (6) with power-law exponent $\nu = \frac{ln1/2}{ln\xi}$. In order to compare the known solution (7) with solution (33),

The number of bars M	The number of the generated points N and value of the cutoff parameter K figuring in (47). N (K)	The value of the constant $A_0^{(2)}$ mimicking the fractal dimension from (47)	The value of the relative error (%)
2	50(12)	-5.35978	0.21354
3	50(12)	-6.36127	0.91534
5	50(12)	-3.77906	1.24461
2	150(22)	-4.98805	1.45124
3	150(22)	-6.92082	0.90255
5	150(22)	-3.57148	0.77035
2	500(33)	-3.77267	12.26469
3	500(33)	-4.80213	6.30386
5	500(33)	-6.40383	6.72678

TABLE 2. The value of the relative error calculated in testing of the hypothesis (47) and (48). See the set of Figures 5, 6, 7 and 8.

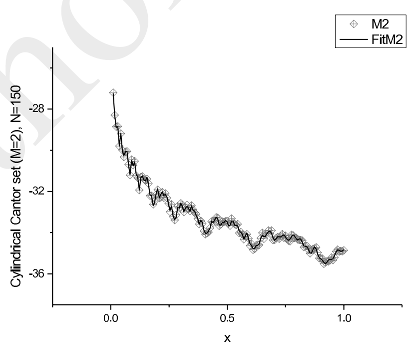

FIGURE 9. The results of the fitting of the function $L_{N_1}(x)$ from (49) to hypothesis (47). The relative error defined by expression (49) equals 1.233%. $\xi = 3/2$.

we present the last one in the form

$$P_{N_1}(z) = PR_\nu(lnz)z^{A_0+RP_2(lnz)},$$
$$RP_2(lnz) = \sum_{k=1}^{\infty}\left[Ac_k\cos(\tfrac{2\pi k}{ln\xi}lnz) + As_k\sin(\tfrac{2\pi k}{ln\xi}lnz)\right]. \qquad (52)$$

The value of N	The value of the cutoff parameter K	A_0
50	9	-1.78077
150	5	-1.71699
150	6	-1.71137
150	7	-1.71105
150	8	-1.70811
150	9	-1.70098
150	10	-1.70497
150	11	-1.70779
150	12	-1.70699
150	13	-1.70976
150	14	-1.70826
150	15	**-1.70971**
200	9	-1.71143
250	9	-1.71159
500	9	-1.71052

TABLE 3. The comparison of the value of the fractal dimension $\nu = \frac{ln(1/2)}{ln(3/2)} = -1.70947...$ with value A_0 at different values of K and N. See expression (51). The closest value to the desired dimension ν is bolded.

From solution (52) it follows that the new solution (32) creates also the log-periodic corrections to the power-law exponent and the constant A_0 should coincide with fractal dimension $\nu = \frac{ln\frac{1}{2}}{ln(\xi)}$. Test calculations realized presumably for N=150 and different values of the cutoff parameter K confirm this relationship. The results of comparison are depicted in Table 3. So, this simple test leads us to one important conclusion: if the microscopic function $f(z)$ from (3) has finite limits for small and large values of z, then the simplest solution (32) allows to find the log-periodic corrections to the fractal dimension coinciding with the constant A_0. This statement is violated when condition (8) is valid.

To conclude this section, let us consider the Cantor set located on the plane XOY and concentrated along two axes. The structure-factor for this case is expressed as [5],

$$P(z_1, z_2) = \prod_{n=-N_1}^{N_1} \left(\frac{\cos(z_1 \xi^n) + \cos(z_2 \xi^n)}{2} \right),$$
$$z_1 = k_x a, \; z_2 = k_y b. \tag{53}$$

A direct application of the approach developed above is impossible because the structure of (53) does not coincide with the structure of the initial product (4). In order to apply this approach, it is necessary to factorize the product (53) and reduce it to a new set of variables. For (53) it can be done easily and the desired product accepts the form

$$P(z_1, z_2) = \prod_{n=-N_1}^{N_1} \left(\cos(\tfrac{z_1+z_2}{2}\xi^n) \cos(\tfrac{z_1-z_2}{2}\xi^n) \right)$$
$$= \prod_{n=-N_1}^{N_1} \left(\cos(\tfrac{z_1+z_2}{2}\xi^n) \right) \prod_{n=-N_1}^{N_1} \left(\cos(\tfrac{z_1-z_2}{2}\xi^n) \right). \tag{54}$$

Now it becomes obvious that this approach can be applied for each product figuring in (54) in separate. From this example one important conclusion follows. If the general structure-factor (product) containing many variables and expressed in the form of expression (3) can be factorized and presented in the form

$$P(z_1, z_2, \cdots, z_r) = \prod_{n=-N_1}^{N_1} f(z_1\xi_1^n) \prod_{n=-N_1}^{N_1} f(z_2\xi_2^n) \cdots \prod_{n=-N_1}^{N_1} f(z_r\xi_r^n), \tag{55}$$

then one can apply the approach developed above to each product figuring in (55).

5. Results and discussions

The approach presented in this paper helps to find new relationships between the procedure of averaging of smooth functions over fractal sets and spatial non-integer integrals. As one can see from the results presented in this paper, this relationship is not simple. If condition (8) is satisfied, then the desired relationship between spatial non-integer integrals that are derived presumably from the structure-factor of type (3) is becoming questionable. In this case there is no direct relationship between the fractal dimension and power-law exponent figuring in the fractional integral. Even in cases when condition (8) is not satisfied, the new approach helps to find the log-periodic corrections (52) for the power-law exponent defining the fractal dimension. Nowadays, many researches try to postulate simply the desired relationship between the fractal structure and the fractional integral and this sincere desire in establishing of this relationship can be violated. This paper can be considered as a specific warning in attempts to impose simply this "obvious" relationship between fractals and non-integer order integrals in space. In next papers we will show that each fractal can generate its specific fractional integral. It is necessary to stress also that the desired original containing convolution of the spatial integral with smooth function in r-space can be obtained from the corresponding Fourier image in k-space by means of expression (3) only approximately. Finishing this section, we want to make two remarks.

REMARK R_1. The first remark is associated with the observation that the linear functional equation (17) is not unique. Other functional equations connecting different $P(z\xi^k)$ are also possible. They can be obtained from any decoupling relationship

$$f(z\xi^{N+k}) = F\Big(f(z\xi^{N+k-1}), f(z\xi^{N+k-2}), \cdots, f(z\xi^{N+1})\Big), \quad (56)$$

where $F(z_1, z_2, \cdots, z_s)$ determines an arbitrary decoupling function of many variables. Of course, in each specific case the selection of the decoupling function $F(z_1, z_2, \cdots, z_s)$ should be justified, explained clearly and tested numerically.

REMARK R_2. The second remark contains the answer for the following question: are there distributions (which are widely used in the mathematical statistics) that can be derived from the product (4) having self-similar properties? At least, one can show three distributions that can be derived from the corresponding functional equations:

(a) Log-normal distribution:

Let us suppose that instead of condition (5) and functional equation (6) we have the following behavior of the microscopic function $f(z)$:

$$\begin{gathered} P(z\xi) = b^{N-|N_0|}\tfrac{f(z\xi^{N+1})}{f(z\xi^{-|N_0|})}P(z),\ \xi > 1, \\ f(z) = Az^{-\alpha} + \cdots (\alpha > 0),\ \text{for } z \gg 1, \\ f(z) = c_0 + c_1 z^{\beta} \cdots (\beta > 0),\ \text{for } z \ll 1. \end{gathered} \quad (57)$$

Taking the natural logarithm from (57) we obtain the following functional equation

$$\begin{gathered} L(z\xi) = L(z) + B - \alpha ln(z), \\ B = (N - N_0)lnb + ln\tfrac{A}{c_0}. \end{gathered} \quad (58)$$

As it was done above in (10), in expression (58) we consider N_0 as a positive value ($N_0 > 0$). The solution of the functional equation (58) has the form

$$\begin{gathered} L(z\xi) = PR_0(ln(z)) + a_1 lnz + a_2 ln^2 z, \\ a_1 = \tfrac{\alpha}{2} + \tfrac{B}{ln\xi},\ a_2 = -\tfrac{\alpha}{2ln\xi}\ \ (\alpha > 0, \xi > 1). \end{gathered} \quad (59)$$

If in expression (57) the constant $c_0 = 0$, then the solution (59) keeps the same form but (in accordance with (57)) it is necessary to make the replacements $c_0 \to c_1$ in (58) and $\alpha \to \alpha + \beta$ in (59), correspondingly. Taking into account the fact that any smooth function taken from the log-periodic function does not change the property of periodicity one can write the solution for *P(z)* from (59) in the form

$$P(z) = PR_0(lnz)\ \exp(a_1 lnz + a_2 ln^2 z). \quad (60)$$

Here the log-periodic function is defined again by relationship (21). In particular case, when $PR_0(lnz) = A_0$ the last expression is reduced to the conventional log-normal distribution.

(b) The χ^2-distribution:

If the microscopic function $f(z)$ has asymptotic behavior of the type

$$f(z) = A\exp(-\gamma z) + \cdots (\gamma > 0),\ \text{for } z \gg 1, \tag{61}$$

then the functional equation for $L(z)$ takes the form

$$L(z\xi) = L(z) + B - \gamma z. \tag{62}$$

Using again an arbitrary constant variation method, it is easy to find the solution for $P(z)$. It is expressed as

$$P(z) = PR_0 ln(z) z^{a_2} \exp(-a_1 z),\ a_1 = \frac{\gamma}{\xi - 1},\ a_2 = \frac{B}{ln\xi}\ (a_{1,2} > 0). \tag{63}$$

In the particular case, when $PR_0(lnz) = A_0$, we obtain from (63) the well-known χ^2-distribution.

(c) The β-distribution:

In the papers [9, 10] it has been proved that the cumulative integral for the strongly-correlated detrended sequences can be described by β-distribution. How to find the fractal (scaling properties) of any two random sequences compared if their β-distributions are remained invariant relatively some linear transformations?

$$x' = ax + b. \tag{64}$$

If we subject the initial β-distribution to the linear transformation then one obtains

$$\begin{aligned} y = A(x - x_0)^\alpha (x_N - x)^\beta + B &\to A(ax - (x_0 - b))^{\alpha'} (x_N - b - ax)^{\beta'} + \tilde{B} \\ &= \tilde{A}(x - \tilde{x_0})^\alpha (\tilde{x_N} - x)^\beta + \tilde{B}, \end{aligned} \tag{65}$$

where

$$\tilde{A} = Aa^{a' + \beta'},\ \tilde{x_0} = \frac{x_0 - b}{a},\ \tilde{x_N} = \frac{x_N - b}{a},\ \tilde{B} = B. \tag{66}$$

As one can see from (65) the β-distribution keeps its invariant properties relatively linear transformations if the power-law exponents of two distributions compared satisfy to the condition

$$\alpha + \beta = \alpha' + \beta' = const = inv. \tag{67}$$

If the power-law exponents and the final points of location of two distribution are known from the fitting procedure (the linear fit of this function is shown in [10]) then the unknown values of linear transformation (a, b) from (64) can be found easily from the relationships (66)

$$a = \frac{x_n - x_0}{\tilde{x_N} - \tilde{x_0}}, \quad b = \frac{x_0 \tilde{x_N} - \tilde{x_0} x_N}{\tilde{x}_N - \tilde{x}_0}. \tag{68}$$

So, we obtain new possibilities for comparison of two random sequences having scaling properties in terms of the invariant properties of β-distribution. If we present this distribution in another form

$$P(z_1, z_2) = A z_1^{\alpha} z_2^{\beta}, \; z_1 = x - x_0, \; z_2 = x_N - x, \tag{69}$$

then one can obtain easily the scaling equation relatively two variables for (68). It has the following form

$$\begin{gathered} L(z_1\xi - z_2\xi) - L(z_1\xi, z_2) - L(z_1, z_2\xi) + L(z_1, z_2) = 0, \\ L(z_1, z_2) = ln[P(z_1, z_2)], \; z_1 + z_2 = x_n - x = const. \end{gathered} \tag{70}$$

So, the functional equations formally containing two variables can be used for investigation of the scaling properties of different fractal systems that cannot be described only in the frame of approach developed above. In conclusion, we want to stress the basic results of the suggested approach:

1. This approach is applicable only in the cases when the structure-factor can be factorized and expressed in the form (55). For other cases, some other approaches can be necessary to apply.

2. This approach is applicable when a current generation of the fractal considered can be expressed in the form of a set of star-vectors in **k**-space. Not all fractals can be expressed in this manner. For random fractals, for example, it is necessary to develop other methods to consider them, in order to establish the desired relationship between some class of fractals and the conventional fractional integrals in space.

3. From this consideration it follows also that the fractal dimension cannot coincide with the power-law exponent figuring in the fractional integral. The log-periodic corrections (expressions (21) and (22)) that follow from the solutions of the functional equations are also possible. They appear in the case when the scaling parameter ξ is distributed over the denumerable set.

6. Mathematical Appendix

The solutions of the functional equation (17).

(See also some results obtained in paper [9]).

1. The solutions of this functional equation are closely related to the well-known solutions of the difference equation of the k-th order with constant coefficients

$$Y_k = a_{k-1} Y_{k-1} + a_{k-2} Y_{k-2} + \cdots + a_0 Y_0. \tag{71}$$

The solution of this equation (when all roots are different) can be written as

$$Y_k = K_1\lambda_1^k + \cdots + K_k\lambda_k^k. \tag{72}$$

If one of the roots is degenerate, then the solution is written as (the integer value g defines the order of degeneracy)

$$Y_k = \left[\sum_{s=1}^{g}(C_s k^{s-1})\right]\lambda_g^k. \tag{73}$$

For both cases the desired roots are found from the polynomial

$$P(\lambda) = \lambda^k - a_{k-1}\lambda^{k-1} - a_{k-1}\lambda^{k-2} - \cdots - a_0 = 0. \tag{74}$$

In complete analogy with these solutions, one can write the general solution of the functional equation (17) for the nondegenerate case (making the formal replacement $K_s \to PR_s(lnz),\ k \to ln(z)/ln(\xi)$,

$$\begin{aligned} L(z) &= \sum_{s=1}^{k} PR_s(lnz)(\lambda_s)^{\frac{lnz}{ln\xi}} = \sum_{s=1}^{k} PR_s(lnz)\exp\left(\tfrac{ln\lambda_s}{ln\xi}lnz\right) \\ &= \sum_{s=1}^{k} PR_s(lnz)z^{\nu_s},\ \nu_s = \frac{ln\lambda_s}{ln\xi}, \end{aligned} \tag{75}$$

and for the case, when one of the roots is g-fold degenerated:

$$L_g(z) = \left[\Sigma_{r=1}^{g} PR_r(lnz)(lnz)^{r-1}\right] z^{\nu_g},\ \nu_g = \frac{ln\lambda_q}{ln\xi}\,. \tag{76}$$

In expressions (75) and (76) the constants K_s are replaced by the log-periodic functions $PR_r(lnz \pm ln\xi) = PR_r(lnz)$, which can be presented by the following decomposition to the Fourier series

$$\begin{aligned} PR_r(z) = A_0^r + \sum_{k=1}^{\infty}\left[Ac_k^{(r)}\cos\left(2\pi k\tfrac{lnz}{ln\xi}\right) + As_k^{(r)}\sin\left(2\pi k\tfrac{lnz}{ln\xi}\right)\right], \\ r = 1, 2, \ldots, k, \ldots. \end{aligned} \tag{77}$$

If one of the roots in (76) is negative, then this root is replaced by its modulus value and the periodic function can be changed for anti-periodic function having the following decomposition

$$\begin{aligned} &PR_r^{(a)}(z) = \sum_{k=1}^{\infty}\left[Ac_k^{(r)}\cos\left(\pi k\tfrac{lnz}{ln\xi}\right) + As_k^{(r)}\sin\left(\pi k\tfrac{lnz}{ln\xi}\right)\right] \quad , \\ &r = 1, 2, \ldots, k,\ PR_r^{(a)}(lnz \pm kln\xi) = (-1)^k PR_r^{(a)}(lnz). \end{aligned} \tag{78}$$

The solution for the complex-conjugated roots is given by expression (22). Other similar functional equations that are reduced to this form are considered in paper [9].

Acknowledgements

This paper was written in the frame of the scientific research program that was accepted by Kazan Federal University for 2013 year "Dielectric Spectroscopy and Kinetics of Complex Systems".

References

[1] D. Baleanu, K. Diethelm, E. Scalas, J.J. Trujillo, *Fractional Calculus Models and Numerical Methods*. Ser. on Complexity, Nonlinearity and Chaos, World Scientific (2012).

[2] A.A. Khamzin, R.R. Nigmatullin, I.I. Popov, B.A. Murzaliev, Microscopis model of dielectric α-relaxation in disordered media. *Fract. Calc. Appl. Anal.* **16**, No 1 (2013), 158–170; DOI: 10.2478/s13540-013-0011-1; http://link.springer.com/article/10.2478/s13540-013-0011-1.

[3] J.A.T. Machado, V. Kiryakova, F. Mainardi, A poster about old history of fractional calculus. *Fract. Calc. Appl. Anal.* **13**, No 4 (2010), 447–454.

[4] J.A.T. Machado, V. Kiryakova, F. Mainardi, Recent history of fractional calculus. *Commun. in Nonlinear Sci. and Numer. Simulation* **16** (2011), 1140–1153.

[5] A. Le Mehaute, R.R. Nigmatullin, L. Nivanen, *Fleches du Temps et Geometrie Fractale*. Paris, Editions Hermes (1998), In French.

[6] R.R. Nigmatullin, A. Le Mehaute, Is there a geometrical/physical meaning of the fractional integral with complex exponent? *J. Non-Cryst. Sol.* **351** (2005), 2888–2899.

[7] R.R. Nigmatullin, Theory of dielectric relaxation in non-crystalline solids: From a set of micromotions to the averaged collective motion in the mesoscale region. *Physica B: Physics of Condensed Matter* **358** (2005), 201–215.

[8] R.R. Nigmatullin, Fractional kinetic equations and universal decoupling of a memory function in mesoscale region. *Phys. A* **363** (2006), 282–298.

[9] R.R. Nigmatullin, Strongly correlated variables and existence of the universal disctribution function for relative fluctuations. *Phys. Wave Phen.* **16**, No 2 (2008), 119–145.

[10] R.R. Nigmatullin, Universal distribution function for the strongly-correlated fluctuations: General way for description of random sequences. *Commun. Nonlin. Sci.* **15** (2010), 637–647.

[11] R.R. Nigmatullin, D. Baleanu, The derivation of the generalized functional equations describing self-similar processes. *Fract. Calc. Appl. Anal.* **15**, No 4 (2012), 718–740; DOI: 10.2478/s13540-012-0049-5; http://link.springer.com/article/10.2478/s13540-012-0049-5.

[12] L. Pietronero, E. Tosatti (Eds.), *Fractals in Physics.* Proc. 6-th Trieste International Symposium on Fractals in Physics, ICTP, Trieste, Italy, July 9-12, 1985, North-Holland (1986).

[13] I. Podlubny, *Fractional Differential Equations.* Academic Press, San Diego (1999).

[14] S.G. Samko, A.A. Kilbas, O.I. Marichev, *Fractional Integrals and Derivatives. Theory and Applications.* Gordon & Breach Sci. Publ., London - N. York (1993).

[15] V.V. Uchaikin, *Fractional Derivatives for Physicists and Engineers.* Ser.: Nonlinear Phys. Sci., Springer (2013).

[1] *Theoretical Physics Department, Institute of Physics*
Kazan Federal University
Kremlevskaya str. 18, 420008, Kazan, RUSSIA
e-mail: renigmat@gmail.com

Received: February 26, 2013

[2] *Department of Mathematics and Computer Sciences*
Faculty of Arts and Sciences
Cankaya University, Ankara, TURKEY
e-mail: dumitru@cankaya.edu.tr

[3] *Department of Chemical and Materials Engineering*
Faculty of Engineering, King Abdulaziz University
Jeddah, SAUDI ARABIA

[4] *Institute of Space Sciences, Magurele - Bucharest, ROMANIA*

Please cite to this paper as published in:
Fract. Calc. Appl. Anal., Vol. **16**, No 4 (2013), pp. xxx–xxx;
DOI:10.2478/s13540-013-0056-1